ARTICLE

IL-34 and protein-tyrosine phosphatase receptor type-zeta-dependent mechanisms limit arthritis in mice

Hilda Minerva González-Sánchez[1,2,9], Jea-Hyun Baek[1,3,9], Julia Weinmann-Menke[4], Amrendra Kumar Ajay[1], Julia Forgan-Farnam Charles[5], Masaharu Noda[6], Ruth Anne Franklin[7,8], Patricia Rodríguez-Morales[7] and Vicki Rubin Kelley[1]✉

Myeloid cell mediated mechanisms regulate synovial joint inflammation. IL-34, a macrophage (Mø) growth and differentiation molecule, is markedly expressed in neutrophil and Mø-rich arthritic synovium. IL-34 engages a newly identified independent receptor, protein-tyrosine phosphatase, receptor-type, zeta (PTPRZ), that we find is expressed by Mø. As IL-34 is prominent in rheumatoid arthritis, we probed for the IL-34 and PTPRZ-dependent myeloid cell mediated mechanisms central to arthritis using genetic deficient mice in K/BxN serum-transfer arthritis. Unanticipatedly, we now report that IL-34 and PTPRZ limited arthritis as intra-synovial pathology and bone erosion were more severe in IL-34 and PTPRZ KO mice during induced arthritis. We found that IL-34 and PTPRZ: (i) were elevated, bind, and induce downstream signaling within the synovium in arthritic mice and (ii) were upregulated in the serum and track with disease activity in rheumatoid arthritis patients. Mechanistically, IL-34 and PTPRZ skewed Mø toward a reparative phenotype, and enhanced Mø clearance of apoptotic neutrophils, thereby decreasing neutrophil recruitment and intra-synovial neutrophil extracellular traps. With fewer neutrophils and neutrophil extracellular traps in the synovium, destructive inflammation was restricted, and joint pathology and bone erosion diminished. These novel findings suggest that IL-34 and PTPRZ-dependent mechanisms in the inflamed synovium limit, rather than promote, inflammatory arthritis.

Laboratory Investigation (2022) 102:846–858; https://doi.org/10.1038/s41374-022-00772-0

INTRODUCTION

Rheumatoid Arthritis (RA) is a common inflammatory autoimmune disease with complex etiologies that target joints. Macrophages (Mø) and neutrophils are prominent in inflamed joints and have been implicated in the pathogenesis of RA. Ample evidence indicates that IL-34, a principle Mø survival and differentiation cytokine, is elevated in the serum, synovial fluid, and synovial cells of patients with RA[1–4]. Despite the notable abundance of IL-34 in RA, the role of IL-34-dependent mechanisms in this illness remains obscure.

IL-34-dependent Mø interacting with neutrophils in the synovium may determine the fate of joint damage in RA. During the effector phase of arthritis, resident Mø are activated and produce chemokines that recruit neutrophils to the inflamed site. Neutrophils readily form highly immunogenic neutrophil extracellular traps (NETs) in RA[5,6]. NETs, subsequently, generate citrullinated modified autoantigens that promote immune responses leading to synovial destruction[7]. Besides forming NETs, neutrophils mediate synovial injury by generating cytotoxic molecules and chemokines that attract Mø to the inflamed synovium[6]. Mø, in turn, may generate molecules that prolong neutrophil survival[8], or alternatively, induce neutrophil apoptosis and subsequently remove them from the synovium[8]. Within the IL-34-rich inflamed joint milieu, it is not clear whether IL-34 drives the expansion of highly plastic and versatile Mø populations to repair or damage tissue. Thus, IL-34-dependent Mø expansion in the inflamed synovium, may either contribute to or, conversely, repress joint damage in RA.

IL-34 and CSF-1 are major Mø growth factors with shared and dissimilar functions. Phenotypically, mice lacking IL-34 are essentially normal[9]. In contrast, CSF-1-deficient mice are plagued by a plethora of immune, reproductive, skeletal, etc. abnormalities[10]. The impact of these cytokines may be related to their receptors. IL-34 and CSF-1 both signal through the CSF-1 receptor (CSF-1R), expressed by Mø, synovial fibroblasts and chondrocytes in RA[11,12]. However, IL-34 also engages a newly identified independent receptor, PTPRZ[13]. While blocking CSF-1R is therapeutic in some arthritic mouse models[14,15], the role of PTPRZ in the pathogenesis of inflammatory arthritis has not been explored.

We investigated whether IL-34 and PTPRZ-dependent Mø and neutrophil interactions promote or suppress inflammatory arthritis. For this purpose, we used K/BxN serum-transfer arthritis[16]. In this model, transferred sera containing Abs against glucose-6-phosphate isomerase (GPI)[17] binds to circulating and pre-existing GPI in the recipient's joints and induces Mø and neutrophil-rich arthritis[16]. The K/BxN serum-transfer arthritis model reflects the

[1]Renal Division, Department of Medicine, Brigham and Women's Hospital, Boston, MA, USA. [2]CONACyT – Centro de Investigación Sobre Enfermedades Infecciosas, Instituto Nacional de Salud Pública, Cuernavaca, Mexico. [3]School of Life Science, Handong Global University, Pohang, Gyeongbuk, Republic of Korea. [4]Department of Nephrology and Rheumatology, University Medical Center of the Johannes Gutenberg University Mainz, Mainz, Germany. [5]Department of Orthopaedic Surgery, Brigham and Women's Hospital, Boston, MA, USA. [6]Homeostatic Mechanism Research Unit, Institute of Innovative Research, Tokyo Institute of Technology, Yokohama, Kanagawa, Japan. [7]Department of Immunology, Harvard Medical School, Boston, MA, USA. [8]Department of Stem Cell and Regenerative Biology, Harvard University, Cambridge, MA, USA. [9]These authors contributed equally: Hilda Minerva González-Sánchez, Jea-Hyun Baek. ✉email: vkelley@rics.bwh.harvard.edu

Received: 8 December 2021 Revised: 2 February 2022 Accepted: 8 February 2022
Published online: 14 March 2022

effector phase of RA; therefore, it is a powerful tool to explore myeloid mechanisms pivotal in this illness. As blocking IL-34 is being considered as a therapeutic in clinical trials for RA, pinpointing the impact of IL-34 and IL-34 receptors during synovial inflammation is timely.

MATERIALS AND METHODS

Mice

C57BL/6 (B6) mice were purchased from The Jackson Laboratory and Harlan Laboratories Inc and non-obese diabetic (NOD) mice from Taconic Biosciences. KRN TCR transgenic mice were a gift from Diane Mathis (Harvard Medical School, Boston, MA). NOD and KRN mice were intercrossed to generate arthritogenic serum from the F1 progeny (K/BxN). Breeding pairs of: (i) Transgenic Tg(Fms-EGFP) reporter mice, expressing EGFP under the control of *Fms* promoter and first intron (MacGreen mice), were provided by D. Hume (Mater Research, South Brisbane, Australia); (ii) PTPRZ KO mice were provided by Masaharu Noda (Tokyo Institute of Technology, Yokohama, Japan)[18]; (iii) IL-34 null LacZ^{+} (IL-34 KO) mice, in which B6 mice were deleted of IL-34 exons 3–5 and intercrossed with IL-34$^{LacZ/+}$ offspring[9] were provided by M. Colonna (Washington University School of Medicine, St. Louis, MO). Use of mice in this study was reviewed and approved by the Standing Committee on Animals in the Brigham and Women's Hospital. Mice with health issues were excluded. We used age-matched male mice 6-10 weeks old, unless otherwise stated.

Serum and synovial tissue specimens

Cohort demographics are listed in Supplemental Table 1. Synovial tissue was provided by the Departments of Pathology and Orthopedics, Medical Center of the Johannes Gutenberg-University Mainz. Specimens were taken from RA patients with a total score ≥6 of 10 from the individual scores in 4 domains using the ACR criteria for RA. Activity and Remission of RA was defined by the Disease Activity Score (DAS). A score <2.6 was defined as remission/low disease activity[19]. All patients provided informed consent. Synovial tissue of RA patients was taken during arthroscopy of the knee/wrist, and in osteoarthritis during hip/knee replacement. Control tissue was taken from patients with pain of unknown origin without a history of autoimmune disease such as RA or chronic joint damage such as OA. Volunteers were screened for health by exclusion of any prior kidney diseases, diabetes, hypertension, and autoimmune diseases. Use of human specimens was reviewed and approved by the Standing Committee for Clinical Studies of the Johannes-Gutenberg University in adherence to the Declaration of Helsinki.

K/BxN serum-transfer arthritis

Serum from K/BxN (eight weeks of age) mice was collected, pooled, and stored at −80 °C. Serum transfer arthritis was induced in IL-34 KO, PTPRZ KO and WT mice by injecting anti-GPI Ab^{+} K/BxN serum (150 µL) on d 0 and 2 (Ref. [17]).

RNA isolation and quantitative PCR

A. Mouse. Total RNA was isolated from synovial tissue using TRIzol (Life Technologies, Carlsbad, CA). Residual DNA was removed by treatment with 1 U of DNase I (Invitrogen, Waltham, MA). Reverse transcription reaction was performed on 100 µg of RNA using an oligo (dT) primer and Superscript II reverse transcriptase (Life Technologies), and relative quantitation with real-time two-step RT-PCR with SYBR Green PCR reagents (Qiagen, Valencia, CA) and an ABI PRISM 7700 sequence detection system (PE Applied Biosystems, Foster City, CA) according to the manufacturer's instructions, as previously described[20]. Primers were purchased from Integrated DNA Technologies. The primer sequences are listed in Supplemental Table 2. The data were analyzed by the ΔΔ-CT method.

B. Human. mRNA from paraffin embedded tissue was isolated with the RNeasy FFPE Kit (Qiagen, Hilden, Germany) according to the manufacturer's guideline. To quantify *CSF1*, *CSF1R*, *IL34* and *PTPRZ* expression we performed quantitative RT-PCR using the "Quantitect Sybr Green PCR Kit" (Qiagen) in combination with the Quantitect Primer Assays (Hs_IL-34_1_SG; Hs_CSF1_1_SG; Hs_CSF1R_1_SG; Hs_PTPRZ1_1_SG). We used *ACTB* as a housekeeping gene (Hs_ACTB_2SG). The following real-time PCR protocol was used: 15 min at 95 °C for initial activation of DNA polymerase, 45 cycles of 15 s at 95 °C, 30 s at 57 °C, 30 s at 72 °C and 30 s at 40 °C for cooling in Roche LightCycler. The data were analyzed by the ΔΔ-CT method.

Western blots

We homogenized synovial tissue (50 µg of total protein) and performed immunoblotting, as previously described[21,22]. We performed SDS–PAGE (10% acryl-amide) and western blotting using the Abs listed in Supplemental Table 3. Images were captured using G Box imaging system (Syngene, Frederick, MD).

Immunoprecipitation (IP)

We performed IP as previously described[21]. Briefly, synovial tissues ($n = 8$ pooled/group) were homogenized in RIPA buffer (50 mM Tris-HCl, 150 mM NaCl, 1% NP-40, 0.5% sodium deoxycholate and 0.1% SDS) containing protease and phosphatase inhibitors. Samples were diluted in IP buffer (20 mM Tris-HCl pH 8.0, 137 mM NaCl, 10% glycerol, 1% NP-40, and 2 mM EDTA containing protease and phosphatase inhibitor cocktails) and 1500 µg of protein was incubated with 2 µg of anti-PTPRZ Ab and 50 µl of TrueBlot Anti-Mouse Ig IP agarose beads (Rockland, Limerick, PA; Cat. 00-8811-25) overnight at 4 °C. We washed the beads four times with IP buffer and eluted immune complexes by adding 1x SDS loading dye and heating at 100 °C for 10 minutes. Proteins were transferred onto 0.2 µm PVDF membrane, and immunoblotting was performed using anti-PTPRZ Ab and anti-IL-34 Ab to detect PTPRZ and IL-34, respectively. Mouse light chain IgG was used as a loading control for IP. Ab details are listed in Supplemental Table 3.

Isolating mouse bone marrow derived Mo and Mø

Mouse bone marrow derived Mø were flushed from femur and tibia. After red blood cell lysis and washing, BM-Mo were selected by using the Monocyte Isolation Kit (Miltenyi Biotech, Auburn, CA; cat.130-100-629). Isolated Mo were lysed in 1x RIPA buffer (containing protease and phosphatase inhibitors). Mø were prepared by plating Mo into 6-well plates in DMEM media containing 10 ng/mL M-CSF (Pepro-Tech, cat. 300-25). The media was changed at day 3 and cell lysates were prepared at day 7.

Isolating human Mo (CD14+) and differentiated Mø

Human peripheral blood lymphocytes were isolated from EDTA blood by density gradient centrifugation. After red blood cell lysis and washing with 1x PBS, CD14 + Mo were enriched by using CD14 MicroBeads (Miltenyi-BioTech, cat. 5151203374), according to the manufacturer's instructions. The isolated cells were lysed in 1x RIPA buffer. To differentiate Mo to Mø, Mo were plated into 6-well plates in DMEM media containing 10 ng/mL M-CSF (Pepro-Tech, Rocky Hill, NJ). The media was changed at day 3 and Mø lysates were prepared at day 7.

Immunohistochemistry

Synovial tissue (human) was fixed in 10% neutral buffered formalin, embedded in paraffin, sectioned (4 µm) and stained for the presence of IL-34, CSF-1 and PTPRZ, as previously detailed[23]. Briefly, antigen retrieval was performed by immersion in citrate buffer followed by blocking endogenous peroxidase activity and nonspecific binding of avidin and biotin. We incubated these sections with the primary and secondary Abs listed in Supplemental Table 3, followed by development with 3′3-diaminobenzidine (Vector; Burlingame, CA).

Gross arthritis pathology (mouse)

Visible paw pathology was scored with a maximum of 12 points that corresponded to the sum of each paw score[17]. Complementing visual pathology, increased ankle thickness, an index of arthritis, was monitored using a caliper (Käfer).

ELISA

A. Mouse. We analyzed serum levels of IL-34, CSF-1, and IgG Abs by ELISA, as previously described[24]. All measurements were made in duplicate. The Abs used are listed in Supplemental Table 3. For anti-GPI Abs ELISA, plates were coated overnight at 4 °C with 5 µg/mL of recombinant mouse GPI-GST (in-house production; GPI-GST-expressing *E. coli* provided by Dr. Diane Mathis, Harvard Medical School) in PBS. The wells were washed 3 times

and blocked for 1 h with 1% BSA in PBS. We added diluted serum samples (1/3000-1/30000) and incubated 1 h (RT), followed by 3 washes with 1% BSA in PBS, and once with PBS. Bound Ig was detected with goat anti-mouse detection Ab conjugated with HRP (Southern Biotechnology, Birmingham, AL; cat. 1030-05, 1/4000 in PBS, 1 h [RT]), washed 3 times with 1% BSA in PBS, and once with PBS. We incubated with TMB substrate (Zymed, San Francisco, CA, cat. 0020-23) and added 1 M H_2SO_4 to stop the reaction. Absorbance was measured at 450 nm.

B. Human. To quantify IL-34 and PTPRZ levels in serum samples were analyzed in duplicate using the human IL-34 ELISA (R&D Systems, Minneapolis, MN) kit and human PTPRZ ELISA kit (Cusabio, Houston, TX) according to the manufacturer's instructions. The Abs used are listed in Supplemental Table 3.

Arthritis histopathology (mouse)

Mouse ankles were dissected to remove skin and outer muscles, fixed with 4% paraformaldehyde for 3 days, rinsed with PBS and decalcified with 20% EDTA for 2-3 weeks until bone was soft and pliable[25]. The decalcified ankles were embedded in paraffin and sections (4 µm) were stained with H&E. Stained sections were blindly evaluated for three global features (exudate, presence of inflammatory cells within the joint space; synovitis, the degree of synovial membrane thickening and inflammatory cell infiltration in the articular and adjacent tissue; and cartilage and bone destruction, including erosion and invasion)[26]. Histological scores were ranked as follows: 0, normal; 1, minimal; 2, mild; 3, moderate; 4, marked; 5, severe[27]. At least four joint sections per mouse were analyzed. The analysis was done by individuals blinded to the experimental groups.

Bone erosion

Forepaws were scanned with an isotropic voxel size of 7 µm on a µCT-35 (SCANCO Medical, Zurich, Switzerland) and 3-dimensional images were generated with manufacturer supplied software using a global threshold for bone/marrow cut-off of 367.8 mg HA/cm^3. Periarticular erosions were scored by an observer blinded to genotype using a semi-quantitative method as previously described[28]. Briefly, four sites in the wrist (ulnar epiphysis and bases of the third, fourth, and fifth metacarpals) were scored for severity of erosion using a scale of 0-3, with 3 indicating the most severe erosion, for a cumulative score of 0-12. The analysis was done by individuals blinded to the experimental groups.

Joint cell digestion

Synovial tissue (four paws per mouse) was dissected, minced, and digested for 1 h at 37 °C in collagenase IV (1 mg/ml, 160 U/mg; Worthington Biochemical, Lakewood, NJ). Single cells were strained in 40 µm cutoff, washed with FACS buffer (PBS, 1% BSA, 1 mM EDTA) and stained for flow cytometry.

Flow cytometry

The Abs used for flow cytometry are listed in Supplemental Table 4. Abs were diluted in FACS buffer. We stained single-cell suspensions for the presence of extracellular antigens (20 min at 4 °C), which we fixed with 2% paraformaldehyde at room temperature for 20 min. We then washed once in Permeabilization Wash Buffer (BioLegend, San Diego, CA). Subsequently, we incubated the cells with Abs for intracellular antigens in Permeabilization Wash Buffer overnight at 4 °C. After washing, cells were analyzed on BD LSR II (BD Biosciences; BD FACSDiva software, Franklin Lakes, NJ) equipped with a high-throughput screening unit and analyzed using FlowJo software. For NET detection, we did not permeabilize.

Adoptive transfer

BM $EGFP^+$ cells isolated from MacGreen:B6 mice were adoptively transferred into the tail vein of IL-34 KO and WT mice at days 7 or 11 of K/BxN serum-transfer arthritis (1×10^7 cells per mouse). Mice were sacrificed 4 h later. Synovium and blood samples were processed to detect $EGFP^+$ cells using flow cytometry.

Thioglycollate-induced peritonitis

Peritonitis was induced in female mice using 1.5 mL of 4% thioglycollate broth (w/o indicator and dextrose; Remel, San Diego, CA) injected (i.p.) into IL-34 KO and WT mice (8 weeks of age). At varying times post-injection, we harvested and analyzed peritoneal cells by flow cytometry.

Clearance of apoptotic cells

We prepared a single cell suspension of splenocytes by mechanical disaggregation of B6 spleen followed by digestion with collagenase IV 1 h at 37 °C. Cells were strained in 40 µm cutoff. Erythrocytes were lysed using ammonium-chloride-potassium lysing buffer (BioSource International, Camarillo, CA), and the remaining cells were washed in PBS. Apoptosis of splenocytes was induced by LPS/TNF-α (25/50 ng/mL) treatment for 48 h and stained with Carboxyfluorescein succinimidyl ester (CFSE) Cell Division Tracker kit (BioLegend), according to manufacturer's instructions. Apoptotic labeled cells were injected (i.p.) along with 1.5 mL of 4% thioglycollate broth into IL-34 KO and WT mice. We harvested peritoneal cells with PBS (10 mL) at 48, 72 and 96 h after injection. The frequency of remaining $CFSE^+$ cells was analyzed by flow cytometry.

In a different approach, neutrophils from IL-34 KO and WT mice (male and female) were isolated from peritoneum at 6 h after thioglycollate injection, induced to undergo apoptosis and labelled with CSFE, as described above. Then, we injected (i.p.) these neutrophils into IL-34 KO and WT mice, in which thioglycollate was administered 48 h earlier. Mice were assigned to receive IL-34 KO or WT apoptotic neutrophils using a random number generator (GraphPad Prism, San Diego, CA). Peritoneal cells were collected and analyzed 3 h later. We analyzed the number and frequency of remaining $CFSE^+$ cells by flow cytometry.

Phagocytosis

BM Mø were differentiated from whole BM for one week in L929-conditioned media. After differentiation, BM Mø were treated with 50 ng/mL TNF-α (BioLegend) + 100 ng/mL IL-34 (BioLegend) for 48 h. Apoptotic neutrophils were stained for 45 min using the pHrodo Deep Red Mammalian and Bacterial Cell Labeling Kit (Invitrogen) before incubation with BM Mø for 3 h. As a negative control, BM Mø were treated with 5 µM Cytochalasin D (Sigma, Saint Louis, MO) for 1 h prior to addition of apoptotic neutrophils. For flow cytometry staining, cells were Fc blocked with anti-CD16/32 and dead cells were stained using the Zombie Aqua Fixable Viability Dye (BioLegend), followed by surface staining for CD64. Samples were processed on the CytoFLEX Flow Cytometer (Beckman Coulter, Brea, CA) and data were analyzed with FlowJo V10 (Tree Star Technologies, Ashland, OR). The Abs used are listed in Supplemental Table 4.

Statistics

Data are expressed as means ± SEM. All statistical analyses were performed using GraphPad Prism software, version 5.0 (GraphPad Software). Normality was tested on all data sets using the Shapiro–Wilk test and sets were subsequently checked for outliers (outlier removal Q = 1%), prior to analysis. To determine differences between two groups data was analyzed using the non-parametric two-tailed Mann–Whitney *U* test, and for more than two groups we analyzed using Kruskal–Wallis test with a Dunn post-test to evaluate *p* values. The detailed information on the number of samples, *p* values, and statistical tests is given in the figure legends.

RESULTS

IL-34 and IL-34 receptors are prominently expressed during K/BxN spontaneous and serum transfer arthritis

K/BxN serum-transfer arthritis is a powerful tool to investigate the effector limb of human inflammatory arthritis. Therefore, we probed for IL-34 and IL-34 receptors expression in this model. As IL-34 and CSF-1, principle Mø growth factors, share several Mø overlapping functions, we analyzed their relative expression in arthritis. First, we probed for IL-34 and CSF-1 expression in K/BxN mice with spontaneous arthritis. Both intra-synovial IL-34 and CSF-1 were elevated in K/BxN arthritic mice compared to normal controls, however IL-34 was more robustly upregulated compared with CSF-1 (Suppl-Fig. S1A, B). Moreover, serum IL-34 was elevated in K/BxN arthritic mice compared with normal controls (Suppl-Fig. S1C). Next, probing for intra-synovial PTPRZ and CSF-1R expression in K/BxN arthritic mice, intra-synovial PTPRZ and CSF-1R were both upregulated in arthritic mice compared with normal controls (Suppl-Fig. S1A, B).

Does transferring arthritis with K/BxN serum faithfully mimic IL-34 and IL-34 receptor findings in the spontaneous disease? We

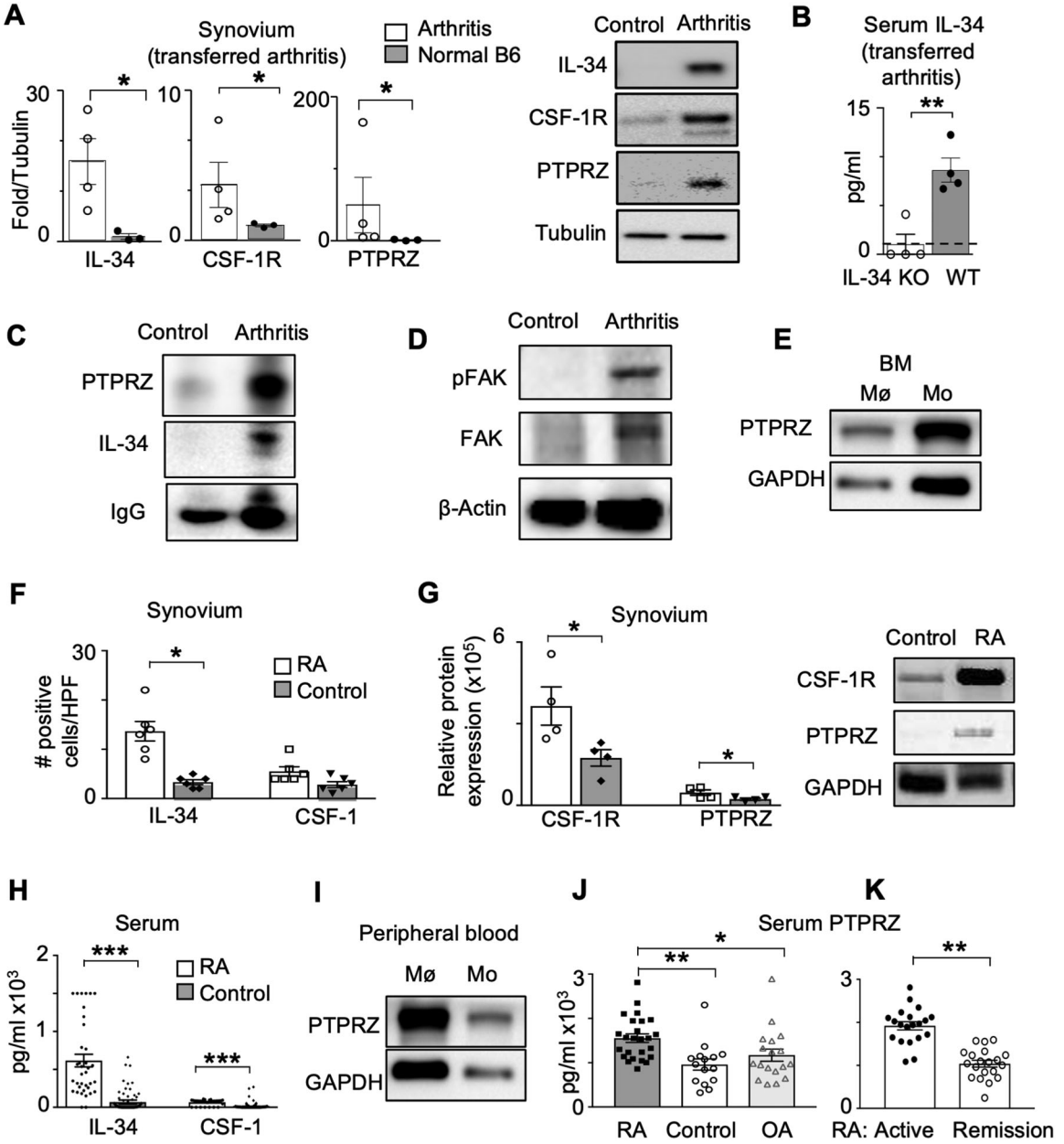

Fig. 1 IL-34 and IL-34 receptors are upregulated in K/BxN serum-transfer mouse inflammatory arthritis and human RA. A Intra-synovial IL-34 and IL-34 receptor expression in arthritic versus normal WT mice [western blots (WB), $n = 3$-4/group]. **B** Serum IL-34 in arthritic WT versus similarly treated IL-34 KO mice (ELISA, $n = 4$/group). WT mouse serum (dotted line). **C** Intra-synovial IL-34 and PTPRZ binding in arthritic versus normal WT mice (Immunoprecipitation, $n = 8$ pooled/group, loading control: IgG). **D** Intra-synovial pFAK and FAK in arthritic versus normal WT mice [WB, same lysates as in **C**, $n = 8$ pooled/group]. **E** PTPRZ in BM derived Mo and Mø (WB, $n = 4$/group). **F** Intra-synovial IL-34 and CSF-1 in RA patients versus controls (immunostaining, $n = 6$/group). **G** PTPRZ and CSF-1R in RA versus controls (WB, $n = 4$/group). **H** Serum IL-34 and CSF-1 in RA versus controls (ELISA, $n = 35$-55/group). **I** PTPRZ in Mø and Mo from healthy controls (WB, $n = 4$/group). **J** Serum PTPRZ in RA versus osteoarthritis (OA) and healthy controls (ELISA, $n = 15$–25/group). **K** Serum PTPRZ levels in active RA versus patients in remission ($n = 20$/group). Panels (**D**, **E**, **G**, **I**), representative of three similar experiments. Data are means ± SEM. $^*P < 0.05$. $^{**}P < 0.01$. $^{***}P < 0.001$; two-tailed, Mann–Whitney *U* test.

detected increased intra-synovial IL-34, CSF-1R and PTPRZ expression and elevated serum IL-34 in K/BxN serum-transfer arthritis compared with untreated controls (Fig. 1A, B, respectively). Importantly, IL-34 binds with PTPRZ (Fig. 1C) and induces focal adhesion kinase (FAK) and phosphorylated FAK (pFAK) signaling (Fig. 1D) in the synovium during arthritis. While it is well established that monocytes (Mo) and Mø ubiquitously express CSF-1R, we identified PTPRZ expression on BM Mo and Mø (Fig. 1E). Collectively, IL-34 and the IL-34 receptors are expressed during K/BxN spontaneous and serum-transfer arthritis in mice.

IL-34 and IL-34 receptor expression in human RA mimics inflammatory arthritis in mice

As the goal is to clarify the role of IL-34 in human RA, we investigated whether the expression of IL-34, CSF-1, and their receptors in human RA parallels mouse K/BxN serum-transfer arthritis. Using synovial tissue from RA patients, we detected a rise in IL-34, CSF-1, CSF-1R and PTPRZ transcripts (Suppl-Fig. S1D) and proteins (Fig. 1F, G, and Suppl-Fig. S1E) compared to synovial tissue from controls (Supplemental Table 1 cohort demographics). Intra-synovial IL-34 expression was greater than CSF-1 in RA

patients (Fig. 1F, Suppl-Fig. S1E, Suppl-Fig. S1D). Consistent with elevated intra-synovial IL-34 and CSF-1 expression in the RA synovium, serum IL-34 and CSF-1 levels were higher in RA compared to healthy controls. (Fig. 1H, Supplemental Table 1 RA cohort demographics). Moreover, IL-34 was higher in active RA patients compared with those in remission (Suppl-Fig. S1G). Thus, intra-synovial IL-34 and CSF-1 expression in human RA and K/BxN serum-transfer arthritis were similar.

Probing for CSF-1R and PTPRZ protein expression, we detected higher intra-synovial CSF-1R compared to PTPRZ expression in RA (Fig. 1G, Suppl-Fig. S1F). Consistent with mouse data, PTPRZ was expressed in human Mo and Mø enriched from peripheral blood (Fig. 1I). Importantly, PTPRZ in the serum was: (i) elevated in RA compared with osteoarthritis (OA) patients and normal controls (Fig. 1J) and (ii) higher in patients with active RA compared to those in remission (Fig. 1K). Collectively, intra-synovial and serum IL-34 and PTPRZ track with RA disease activity in patients and were similarly expressed in human and mouse arthritis.

Arthritis is more severe in IL-34 and PTPRZ KO compared with WT mice

We previously showed IL-34 KO mice were protected from chronic kidney disease[24], while others reported blocking CSF-1R reduced the severity of experimental arthritis[14,15]. Thus, we initially hypothesized that IL-34 promotes inflammatory arthritis. Unexpectedly, we found that arthritis was far more severe in IL-34 KO compared with WT mice. Intra-synovial gross (Fig. 2A, B and Suppl-Fig. S2A) and histopathology (Fig. 2C, D) were worse in IL-34 KO compared to WT mice. Consistent with worse joint pathology, circulating IgG, an index of the severity of arthritis, was elevated in IL-34 KO compared with WT mice (Suppl-Fig. S3A). Moreover, serum anti-GPI Ab levels were similar in IL-34 KO and WT mice, indicating that differing transferred pathogenic Abs levels were not responsible for increasing the severity of arthritis (Suppl-Fig. S3B). Importantly, serum CSF-1 levels did not differ in IL-34 KO and WT mice, suggesting CSF-1 did not compensate for the absence of IL-34 (Suppl-Fig. S3C).

To determine whether IL-34 and PTPRZ-dependent mechanisms similarly limit arthritis, we compared K/BxN serum transfer arthritis in IL-34 and PTPRZ KO with WT mice (Fig. 2A). We found that gross visible pathology was similar in PTPRZ, and IL-34 KO mice, and both were worse than WT mice (Fig. 2B and Suppl-Fig. S2B). As in IL-34 KO mice (Fig. 2C), histopathology was worse in PTPRZ KO compared with WT mice (Fig. 2E, F). Bone erosion is a hallmark of severe RA[29]. To determine the extent of arthritis we used radiology to compare the bones between experimental groups. Bone erosion was more advanced in IL-34 and PTPRZ KO compared with WT mice (Fig. 2G). Finally, we excluded the possibility that IL-34 and PTPRZ KO joints were abnormal prior to inducing arthritis, as IL-34 KO, PTPRZ KO and WT joints were histologically normal (Suppl-Fig. S4). Collectively, PTPRZ and IL-34-dependent mechanisms limited the severity of arthritis.

IL-34 and PTPRZ suppress the intra-synovial accumulation of neutrophils in arthritis

To identify the intra-synovial leukocyte populations that accumulated in IL-34 and PTPRZ KO mice, we analyzed leukocytic subsets during K/BxN serum-transfer arthritis (Fig. 3A). We detected more intra-synovial leukocytes, notably myeloid cells, in IL-34 KO compared with WT mice (Fig. 3B, C). Neutrophils, Mø and T cells were prominent in the inflamed synovium, while B cells were far lesser (Fig. 3D–G). The frequency and number of intra-synovial neutrophils and Mø were more robust in IL-34 KO compared with WT mice (Fig. 3D, E), while the rise in neutrophils was higher compared with Mø. We detected similar numbers of intra-synovial T cells in IL-34 KO compared with WT mice (Fig. 3F). Thus, a prominent rise in the accumulation of neutrophils was detected in the absence of IL-34 during arthritis.

As PTPRZ is expressed in the inflamed synovium and on Mø[24], we repeated the above experiments comparing PTPRZ KO and WT mice (Fig. 3H). Consistent with the rise in total leukocytes, myeloid cells were elevated in PTPRZ KO compared with WT mice (Fig. 3I–K). As in IL-34 KO mice, neutrophils were more abundant than Mø (Fig. 3L) in PTPRZ KO compared with WT mice, whereas the number of T and B cells were similar in both groups (Fig. 3M, N). Taken together, IL-34 and PTPRZ-dependent mechanisms suppress the intra-synovial accumulation of neutrophils during inflammatory arthritis.

IL-34 suppress the accumulation of NETs in the synovium in arthritis

NETs are released by neutrophils during synovial injury, and are common in the joints of RA patients[7]. NETs modulate innate and adaptive immune responses leading to tissue injury[7] and articular cartilage damage[5]. As synovial pathology and bone erosion are increased in IL-34 KO, we hypothesized that NETs are more abundant in the absence of IL-34 during arthritis. We detected more intra-synovial NETs in IL-34 KO compared with WT mice during arthritis (Fig. 4A, B). Thus, IL-34-dependent mechanisms restrict NET accumulation in the inflamed synovium during arthritis.

Why do more neutrophils and NETs accumulate in the synovium of IL-34 KO mice compared to WT mice? We hypothesized that IL-34 reduces intra-synovial neutrophil recruitment and NETs. To test this, we used a EGFP reporter for CSF-1R, MacGreen mice. In this transgenic strain, Mø and neutrophils express fluorescent CSF-1R and can be tracked[30]. We injected $EGFP^+$ BM cells into recipient IL-34 KO and WT mice with arthritis (day 11). After 4 h, we analyzed $EGFP^+$ donor cells in the synovium (Suppl-Fig. S5A). $EGFP^+$ circulating cells were equivalent, as there were similar numbers in IL-34 KO and WT blood (Suppl-Fig. S1B, C). Notably, more $EGFP^+$ neutrophils, not Mø, were recruited to IL-34 KO compared to WT synovium (Suppl-Fig. S5D, E). Next, we tracked the intra-synovial accumulation of NETs formed from neutrophils (Fig. 4C). We identified more $EGFP^+$ BM cells (Fig. 4D), largely neutrophils (Fig. 4E), not Mø (Fig. 4G), in the IL-34 KO compared with WT synovium. Importantly, there were more intra-synovial $EGFP^+$ NETs in IL-34 KO compared with WT mice (Fig. 4F). Thus, enhanced intra-synovial neutrophil recruitment leads to greater accumulation of NETs in mice lacking IL-34 during arthritis.

Chemokines recruit neutrophils into the inflamed synovium and promote RA[31,32]. We explored whether IL-34 suppresses intra-synovial chemokine expression, linked to RA, during K/BxN serum-transfer arthritis. Chemokines, known to recruit neutrophils, albeit some along with other leukocyte populations, were elevated in IL-34 KO mice (Fig. 4H, I). Therefore, IL-34-dependent mechanisms suppress chemokines that attract neutrophils into the inflamed synovium, and thereby limit the severity of destructive inflammation.

IL-34 leads to enhanced clearance of apoptotic neutrophils

It could be argued that increased intra-synovial neutrophils, NETs and chemokines may be a consequence of heightened inflammation in IL-34 and PTPRZ KO mice. Therefore, we probed more deeply into the Mø mediated mechanisms central to IL-34 and PTPRZ suppressing inflammation. As impaired clearance of dying cells is pathogenic during arthritis[33], we hypothesized that IL-34 enhances Mø-mediated clearance of apoptotic neutrophils, and thereby dampens arthritis. It was not feasible to introduce apoptotic neutrophils into the synovium to track clearance. Thus, we used thioglycollate-induced peritonitis model as (i) ample amounts of labeled apoptotic cells could be delivered to monitor clearance and (ii) IL-34 protein, not CSF-1, was abundantly expressed in peritoneal fluid (Suppl-Fig. S6). In thioglycollate-induced peritonitis, neutrophils peak within hours and are essentially undetectable by 48 h, the peak time for Mø accumulation. During peritonitis, we detected similar numbers of

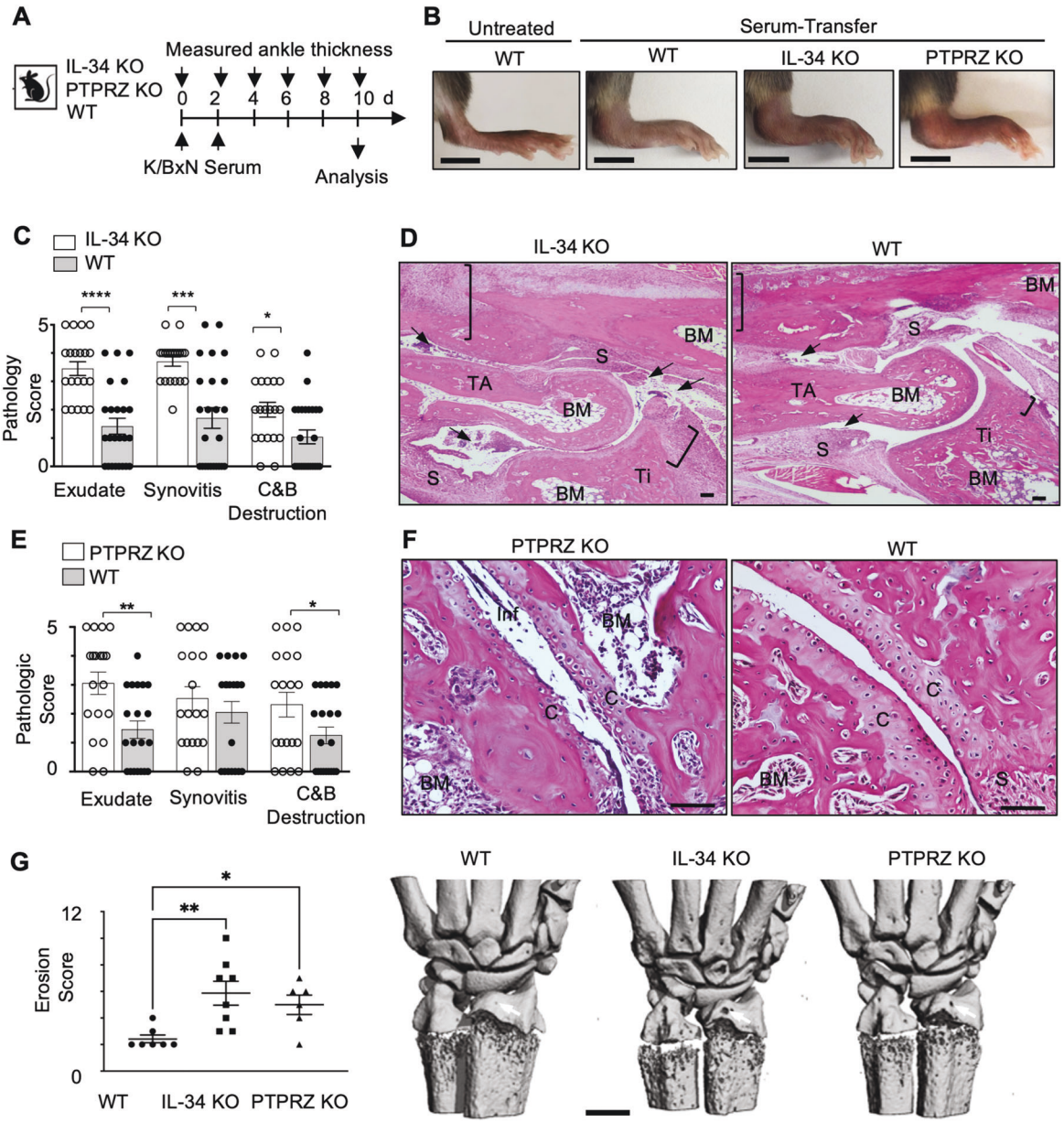

Fig. 2 IL-34 and PTPRZ gene deletion exacerbates K/BxN serum-transfer arthritis. A Experimental scheme. **B** Representative pictures of IL-34 KO, PTPRZ KO and WT hind limbs in arthritic and untreated normal WT (scale bar = 0.5 cm). **C** Histopathology score assessed in arthritic IL-34 KO and WT cross sectioned joints (4 µm, $n = 20$-24 joints/group [5-6 mice/group]). **D** Representative IL-34 KO and WT arthritic joint H&E sections (day 10, scale bar = 200 µm). **E** Histopathology score assessed in arthritic PTPRZ KO and WT cross-sections (4 µm, $n = 20$ joints/group [five mice/group]). **F** Representative PTPRZ KO and WT arthritic joint H&E sections (day 10, scale bar = 100 µm). For panels (**D**) and (**F**): arrows, infiltrates in the joint space (exudate); brackets, articular and adjacent tissue inflammation; BM bone marrow, C cartilage, Inf infiltrates, S synovium, Ti tibia, and TA talus. **G** Bone erosion evaluated using micro-CT scans ($n = 6$–8/group). Photos: Scale bar = 0.5 mm, white arrows, erosions on each of the ulnar epiphyses. Data are means ± SEM. Two-tailed Mann–Whitney *U* test (**C**, **D**) or Kruskal–Wallis test with a Dunn post-test (**E**). $^{*}P < 0.05$. $^{**}P < 0.01$. $^{***}P < 0.001$. $^{****}P < 0.0001$.

intra-peritoneal Mø in IL-34 KO and WT mice (Fig. 5A, B). To determine whether IL-34 enhances Mø clearance of apoptotic neutrophils, we induced peritonitis and injected CFSE-labeled apoptotic neutrophils into the peritoneum 48 h later. We compared donor apoptotic neutrophils generated from IL-34 KO and WT (Fig. 5C) and analyzed the frequency of CFSE-labeled neutrophils in IL-34 KO and WT mice 3 h later (Suppl-Fig. S7). Irrespective of the source of the apoptotic neutrophils, the number and frequency (Fig. 5D) of apoptotic neutrophils in the inflamed peritoneum was higher in IL-34 KO compared with WT mice. After normalizing the ratio of apoptotic neutrophils cleared by Mø, we concluded that IL-34 KO Mø were defective in removing apoptotic neutrophils (Fig. 5E). Moreover, defective IL-34 KO Mø clearance was not limited to apoptotic neutrophils, as the clearance of apoptotic splenocytes during peritonitis was reduced in IL-34 KO compared to WT mice (Suppl-Fig. S8).

To determine whether IL-34 signaling through PTPRZ likely limited the severity of arthritis, we compared apoptotic neutrophils clearance in IL-34 KO, PTPRZ KO, and WT mice (Fig. 5F). More apoptotic neutrophils were detected in IL-34 and PTPRZ KO compared to WT mice (Fig. 5G). Normalizing the ratio of apoptotic neutrophils removed by Mø, as above, the clearance of apoptotic neutrophils was reduced in IL-34 and PTPRZ KO mice compared to WT (Fig. 5H). Consistent with this data, in vitro phagocytosis of

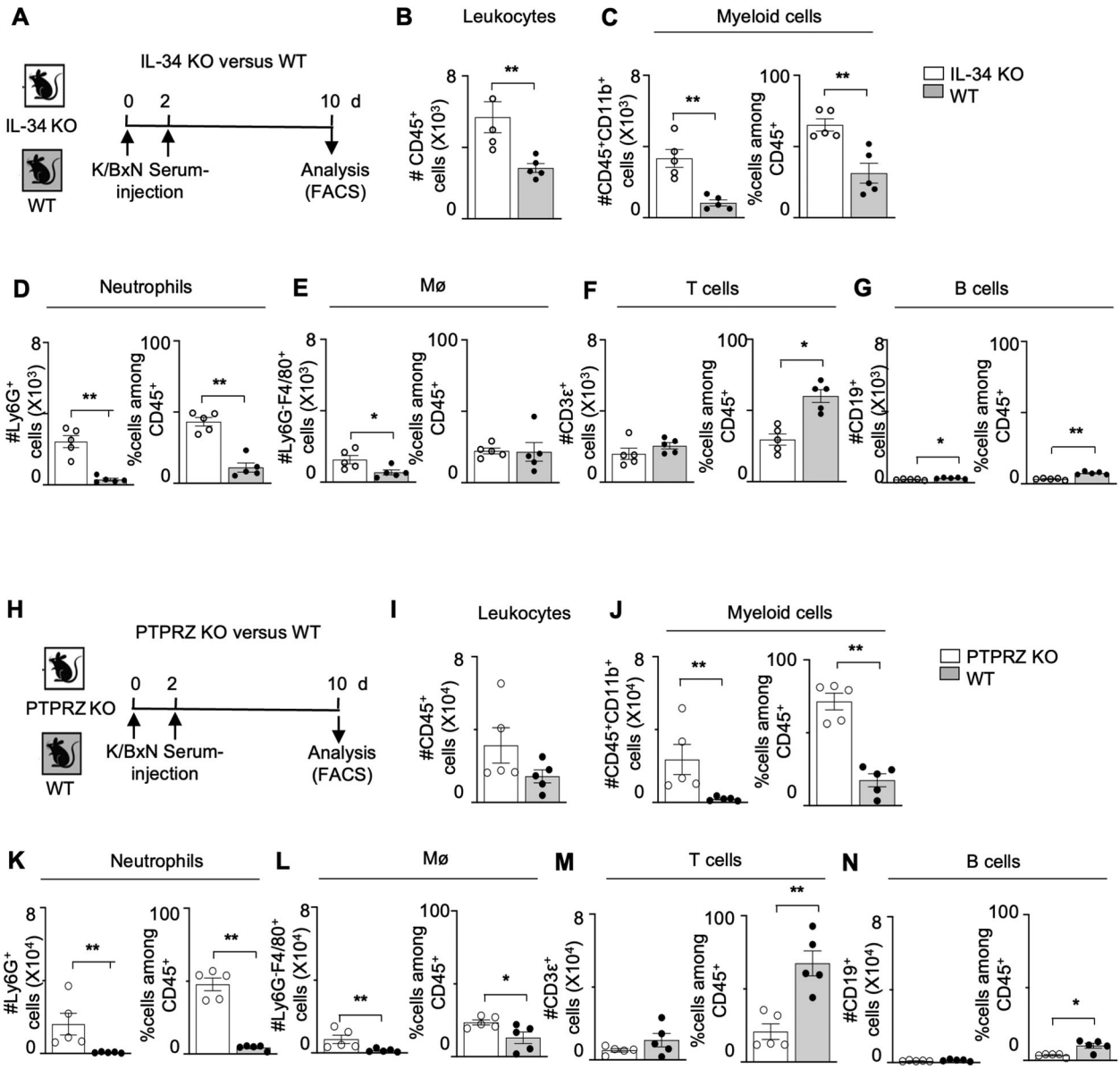

Fig. 3 More leukocytes, predominately myeloid cells, accumulate in the synovium of IL-34 KO and PTPRZ KO with K/BxN serum-transfer arthritis versus WT mice. A Experimental scheme for the analysis of leukocytes subsets in IL-34 KO versus WT in synovial tissue. **B**–**G** Synovial tissue was analyzed and compared in IL-34 KO and WT mice after the induction of arthritis (day 10) using relevant markers by flow cytometry. Representative of four similar experiments. **B** Number of leukocytes. Number and frequency of (**C**) myeloid cells, (**D**) neutrophils, (**E**) Mø, (**F**) T cells, and (**G**) B cells in IL-34 KO and WT synovium. **H** Experimental scheme for the analysis of leukocytes subsets in PTPRZ KO versus WT in synovial tissue. **I**–**N** Synovial tissue analyzed in PTPRZ KO and WT mice after the induction of arthritis (day 10) by flow cytometry. Representative of four similar experiments. **I** Number of leukocytes. Number and frequency of (**J**) myeloid cells, (**K**) neutrophils, (**L**) Mø, (**M**) T cells, and (**N**) B cells in PTPRZ KO and WT synovium. Data are represented as the means ± SEM ($n = 5$/group). *$P < 0.05$. **$P < 0.01$; two-tailed, Mann–Whitney U test.

apoptotic neutrophils was defective in PTPRZ KO, and to a lesser degree, IL-34 KO, BM Mø, albeit Mø phagocytosis in vitro may not necessarily recapitulate in vivo findings (Suppl-Fig. S9). Collectively, this suggests that IL-34 and signaling via PTPRZ enhances Mø clearance of apoptotic neutrophils, and in turn, contributes to limiting the severity of arthritis.

IL-34 and PTPRZ-dependent mechanisms skew Mø towards a reparative phenotype

Mø skewed towards a reparative phenotype, ("M2" Mø), are powerful phagocytes. We found that IL-34 and PTPRZ Mø promote the clearance of apoptotic neutrophils. Therefore, we hypothesized that IL-34 and PTPRZ-mediated mechanisms skew Mø towards a highly phagocytic Mø phenotype, and thereby restrict joint inflammation during RA. We found that intra-synovial Mø expressing: (i) CD163, a scavenger receptor prominent in resolving inflammation, and (ii) CD301, a marker of "M2" Mø, were reduced in IL-34 and PTPRZ KO mice during K/BxN serum induced arthritis (Fig. 6A–C). Moreover, we detected more Ly6C^{hi} Mø and intra-synovial Mø expressing TNF-α and iNOS, destructive Mø (often referred to as "M1" Mø) in IL-34 and PTPRZ KO compared to WT mice (Fig. 6E, F). Similarly, we identified more IL-10^{+}Mø, that dampen inflammation, in IL-34 and PTPRZ KO compared with WT mice (Fig. 6F). While an expansion of locally renewing resident Mø expressing CX3CR1 restrict joint inflammation[34], we did not detect a difference in the number of this population in IL-34 and PTPRZ

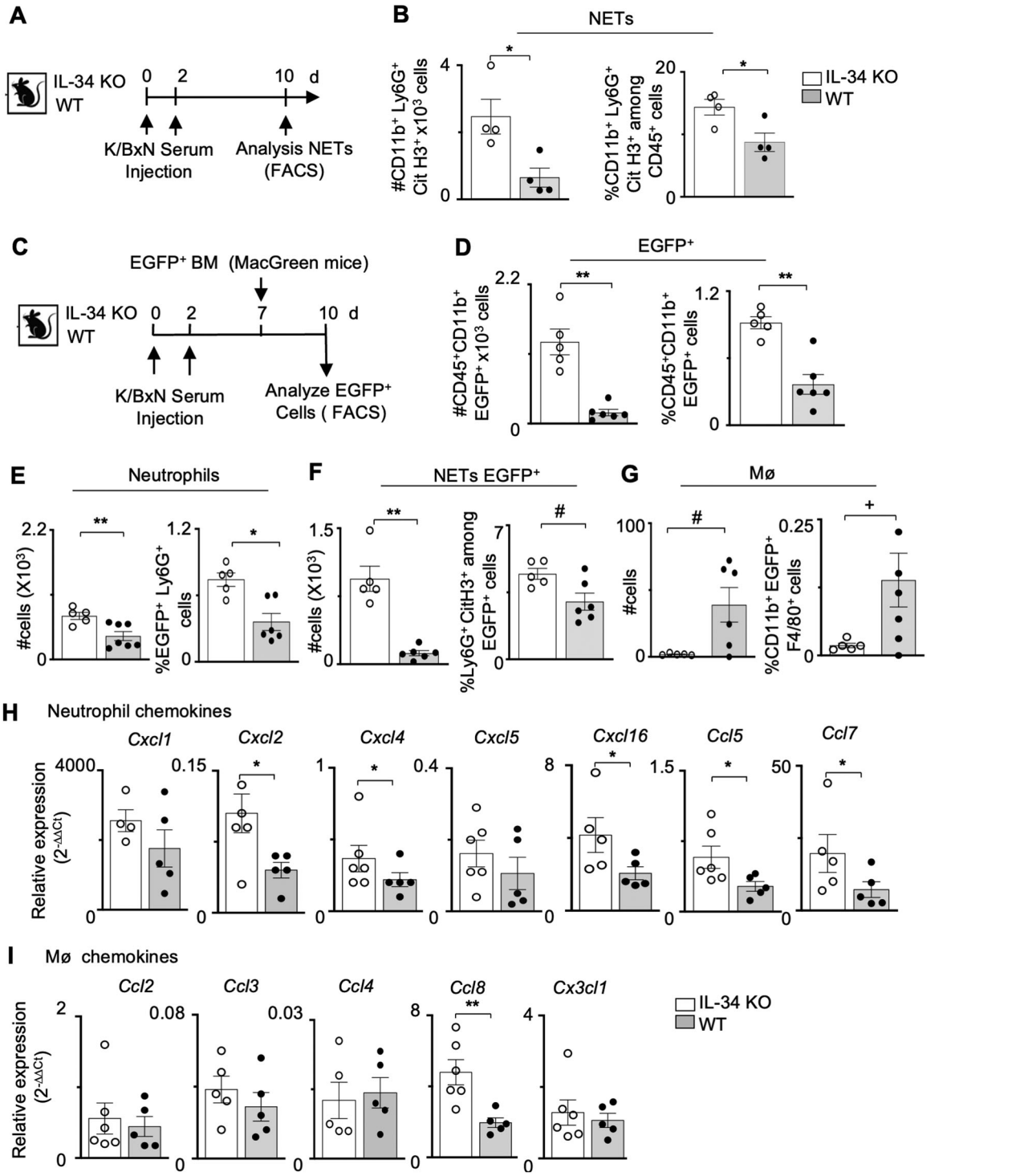

Fig. 4 IL-34 deletion increases intra-synovial NETs in K/BxN serum transfer arthritis. A Experimental scheme. Synovial tissue was analyzed for neutrophils expressing, a key early NETosis marker (citrullinated histone H3 [Cit H3]), after inducing arthritis in IL-34 KO and WT mice using flow cytometry. **B** Number and frequency of neutrophils expressing Cit H3 in IL-34 KO and WT detected by flow cytometry ($n = 4$/group). Representative of two similar experiments. **C** After inducing arthritis, we injected (iv) MacGreen BM ($EGFP^+$) cells into IL-34 KO and WT mice (day 7). After sacrificing (day 10) synovial tissue was analyzed for infiltrating $EGFP^+$ cells expressing Cit H3 by flow cytometry (Scheme). Number and frequency of total $EGFP^+$ cells (**D**), $EGFP^+$ neutrophils (**E**), $EGFP^+$ NETs (identified by the expression of Cit H3) (**F**), and $EGFP^+$ Mø (**G**); using relevant markers by flow cytometry ($n = 5$–6/group). **H**, **I** Intra-synovial chemokine transcripts were analyzed using qPCR in IL-34 KO and WT mice after inducing arthritis (d8, $n = 4$-6/group). Chemokine expression is displayed for chemokines that recruit neutrophils (**H**), and chemokines that recruit Mø (**I**). Data are represented as the means ± SEM. $^{\#}P < 0.08$. $^{+}P < 0.06$. $^{*}P < 0.05$. $^{**}P < 0.01$; two-tailed, Mann–Whitney *U* test.

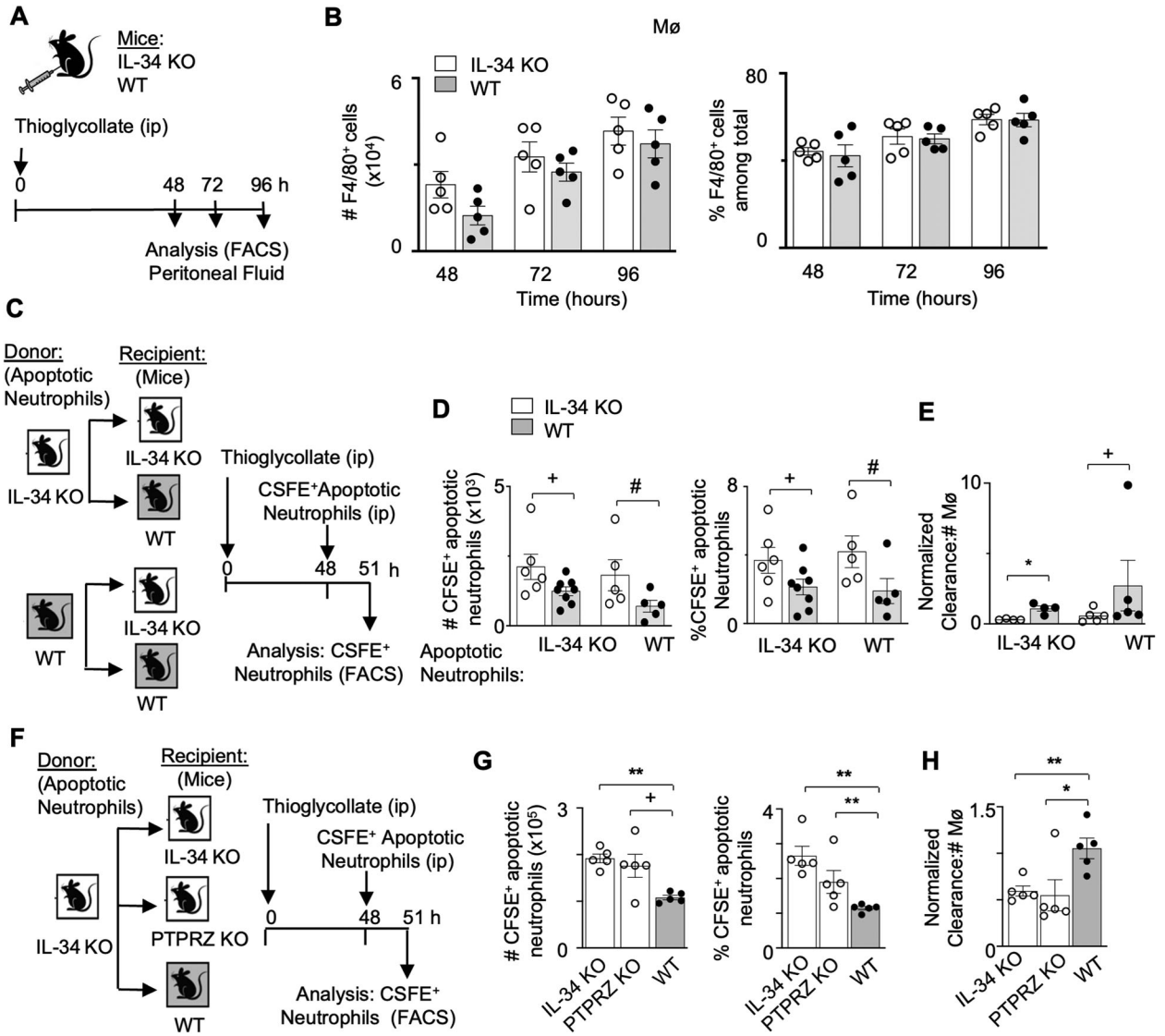

Fig. 5 Clearance of apoptotic cells is suppressed in IL-34 KO during peritonitis. A Experimental scheme. **B** Number and frequency of Mø in the peritoneal fluid (PF) after inducing peritonitis (48, 72, and 96 h) (flow cytometry, $n = 5$/group). Representative of two experiments. **C** Experimental scheme: CSFE-labeled apoptotic neutrophils (2.5×10^6) generated from IL-34 KO and WT donors were injected (i.p.) into IL-34 KO and WT recipient mice 48 h after inducing peritonitis. Remaining $CFSE^+$ cells were analyzed 3 h later by flow cytometry. **D** Number and frequency of CFSE-labeled neutrophils in the PF (flow cytometry, $n = 5$–8/group). **E** Normalized ratio of apoptotic neutrophils cleared by Mø in PF (averaged # remaining apoptotic neutrophils in B6 mice/ remaining apoptotic neutrophils, divided by # Mø in each sample/ averaged # Mø in B6 mice). **F** Experimental scheme for the clearance of apoptotic neutrophils (CSFE-labeled, IL-34 KO donors, 2.5×10^6 cells) analyzed as in (**C**). **G** Number and frequency of CFSE-labeled neutrophils in PF (flow cytometry, $n = 5$/group). **H** Normalized ratio of the number of apoptotic neutrophils cleared by Mø (calculated as in **E**). Data are represented as the means ± SEM. $^{\#}P < 0.09$. $^{+}P < 0.08$. $^{*}P < 0.05$. $^{**}P < 0.01$; 2-tailed, Mann–Whitney *U* test.

KO compared with WT mice (Fig. 6D). Collectively, this suggests that IL-34 and PTPRZ-dependent mechanisms expand Mø populations that remove dying neutrophils, and thereby restrict destructive joint inflammation.

In conclusion, these novel findings indicate that IL-34 and PTPRZ-dependent mechanisms promote the expansion of Mø that limit intra-synovial inflammation and, thereby arthritis in mice (graphic mechanistic details in Fig. 7).

DISCUSSION

We now report that IL-34 and PTPRZ are upregulated in the synovium during mouse inflammatory arthritis and human RA. Moreover, IL-34 binds to PTPRZ and induces pFAK signaling, a tyrosine kinase known to regulate cell adhesion, proliferation, differentiation, and motility. Using the K/BxN serum-transfer arthritis, IL-34 and PTPRZ expression was protective, as arthritis was more severe in IL-34 and PTPRZ KO compared to WT mice. Mechanistically, IL-34 and PTPRZ enhance Mø clearance of apoptotic neutrophils and thereby decrease neutrophils and NETs accumulating in the synovium. With fewer neutrophils and NETs accumulating in the synovium, destructive inflammation was restricted leading to diminished pathology and bone erosion (Fig. 7). These novel findings indicate that IL-34 and PTPRZ-dependent mechanisms promote the expansion of Mø that restrict intra-synovial inflammation and in turn, arthritis.

We found that in the absence of IL-34 intra-synovial neutrophil recruitment and neutrophil and NET accumulation increased in

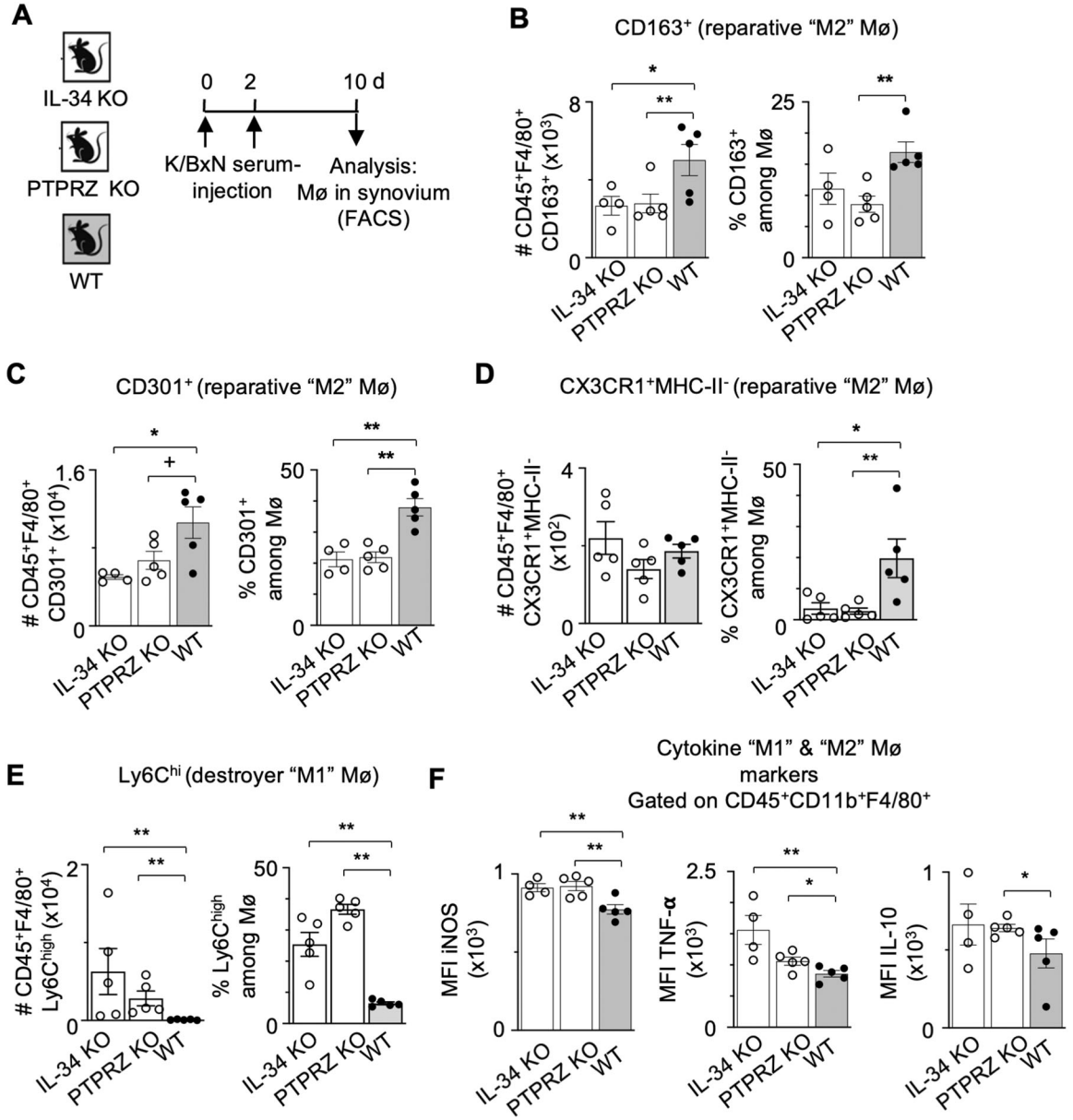

Fig. 6 IL-34 and PTPRZ-mediated mechanisms skew Mø towards a reparative "M2" phenotype in the synovium during K/BxN serum-transfer arthritis. A Experimental scheme for the analysis of destroyer "M1" and reparative "M2" markers in IL-34, PTPRZ KO and WT in synovial tissue by flow cytometry. **B**–**D** Reparative "M2" Mø markers in synovial tissue of IL-34, PTPRZ KO and WT mice after induction of arthritis (day 10). Representative of two similar experiments. **B** Number and frequency of $CD163^+$ Mø. **C** Number and frequency of $CD301^+$ Mø myeloid cells. **D** Number and frequency of $CX3CR1^+MHC\text{-}II^-$ Mø. **E** Inflammatory destroyer "M1" Mø detected by the high expression of Ly6C in synovial tissue of IL-34, PTPRZ KO and WT mice after induction of arthritis (day 10). Representative of two similar experiments. **F** Mean Fluorescent Intensity (MFI) of relevant cytokine Mø destroyer "M1" markers, (iNOS, TNF-α) and IL-10 in synovial Mø of IL-34, PTPRZ KO and WT mice. Data are represented as the means ± SEM ($n = 4$–5/group). $^+P < 0.07$. $^*P < 0.05$. $^{**}P < 0.01$; two-tailed, Mann–Whitney *U* test.

arthritis. As neutrophils do not express the CSF-1R protein[30], nor *Ptprz* and *Sdc1* transcripts[35] (public data, Immunological Genome Project), it is improbable that IL-34 directly suppresses neutrophils in the inflamed synovium. More plausibly, the absence of IL-34 indirectly leads to enhanced inflammation and, thereby, a greater expression of chemokines that recruit neutrophils into the inflamed synovium. In this regard, we detected a higher intra-synovial expression of neutrophil-attracting chemokines in IL-34 KO mice with induced arthritis. Adding translational credence to this finding, the same chemokines are abundant in the serum and synovial fluid in RA patients[31,32]. Notably, these elevated chemokines not only act as chemo-attractants, but functionally contribute to the pathogenesis of RA[31,36]. As NETs orchestrate immune responses leading to inflammation[7] and cartilage damage[5], without IL-34 to reduce NETs, joint damage was more severe. Collectively, IL-34-dependent mechanisms reduce intra-synovial neutrophil recruitment indirectly, via suppressing chemokines and subsequently hindering neutrophil and NET accumulation, and in turn, joint damage in K/BxN serum-induced arthritis.

The burning issue is to identify the direct IL-34-dependent steps that suppress arthritis. We found that apoptotic neutrophils and NETs are more prevalent and promote induced arthritis in the absence of IL-34. As many forms of physiological cell death

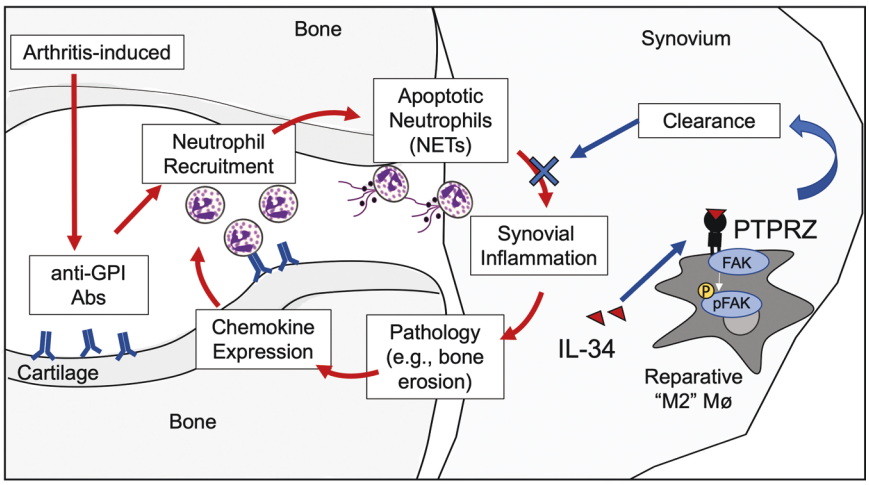

Fig. 7 IL-34 and PTPRZ-dependent mechanisms limit arthritis in mice. During arthritis, myeloid-mediated mechanisms escalating joint damage include: (i) elevated anti-GPI Abs that recruit and activate neutrophils; (ii) intra-synovial short-lived activated neutrophils that lead to apoptotic neutrophils and NETs accumulation; and (iii) NETosis inducing neutrophil-specific chemokines in the synovium that recruit more neutrophils that form NETs and thereby drive cyclical joint destruction. However, IL-34 signaling through PTPRZ polarize Mø to M2 "healers" that enhance clearance of apoptotic neutrophils and NETs, thereby, limiting arthritis. With fewer neutrophils and NETs accumulating in the synovium, destructive inflammation was restricted, and in turn, joint pathology and bone erosion was diminished.

generate antigens that often lead to harmful autoimmune responses[37], efficient removal of apoptotic neutrophils and NETs is central to limiting tissue damage[38]. Therefore, we hypothesized that IL-34-dependent clearance of dying neutrophils hinders escalating synovial damage in RA. We now report that IL-34 and PTPRZ enhance efferocytosis of apoptotic neutrophils during Mø-rich acute inflammation. In our study, Mø are responsible for efferocytosis as they were the predominant leukocytes in the peritoneum during the assay, phagocytose apoptotic neutrophils during inflammation[39], and our Mø in vitro phagocytosis data is consistent with the in vivo findings. Elevated apoptotic neutrophil clearance occurs similarly using IL-34 KO and WT apoptotic neutrophils, thereby excluding the possibility of IL-34-mediated enhanced "eat-me" signals. Thus, IL-34 and PTPRZ promote Mø that remove dying neutrophils and thereby suppress synovial damage in K/BxN serum-transfer arthritis.

We report the novel finding that intra-synovial IL-34 skews hematopoietic cells toward a joint protective, healer, phenotype. The synovium contains both pathologic and joint-protective Mø[14,15,34,40,41]. How does IL-34 skew Mø to enhance healing in during inflammatory arthritis? IL-34 may directly expand Mø populations geared to quench intra-synovial inflammation. In support of this concept, Mø in the presence of IL-34 in vitro acquire a healer phenotype[42,43], that are highly phagocytic[44]. We showed intra-synovial, BM derived Mø with a reparative phenotype are diminished and inflammatory destructive phenotype Mø are more abundant in the absence of IL-34 and PTPRZ during arthritis. Collectively, we suggest that IL-34, engaging with intra-synovial Mø, expressing PTPRZ, promotes the clearance of apoptotic neutrophils, thereby limiting the severity of arthritis.

The inflamed microenvironment dictates whether IL-34 expression is beneficial or harmful. We originally hypothesized that IL-34 deficiency suppresses RA as our prior studies showed reduced acute and chronic kidney disease in IL-34 KO mice[20,24]. Moreover, as IL-34 is elevated in patients with RA, it was considered to be harmful. Consistent with this: (i) IL-34 promotes tumor progression[45], and (ii) injecting systemically IL-34 exacerbates arthritis (collagen-induced)[46]. However, we found that K/BxN serum-induced arthritis was far more severe in IL-34 KO mice. Akin to our findings, IL-34: (i) protects neurons in a model of Alzheimer disease by promoting microglia proliferation and clearance of oligomeric amyloid-β[47], (ii) improves bacterial clearance in a model of sepsis[48], and (iii) promotes allograft tolerance by inducing tolerogenic Mø and Tregs[49]. As the microenvironment differs in varying animal models, tissues and stages of inflammation, the local milieu likely determines whether IL-34 is harmful or beneficial. Moreover, we wish to emphasize that the data in RA patients showing that IL-34 increases during disease progression is limited. These findings were based on an association, in vitro experiments[2,3,50–52] and lack mechanistic data[1,4,53,54]. Clearly, it is critical to clarify the IL-34-dependent mechanisms, within the context of inflamed joint microenvironment, prior to translating findings into therapeutic strategies for human RA.

We report the novel finding that signaling through PTPRZ limits arthritis. Unlike CSF-1 that solely binds to CSF-1R, IL-34 engages CSF-1R along with two other receptors, PTPRZ and syndecan-1 (SDC-1). These receptors engage IL-34 differently, PTPRZ binds IL-34 independently[13], while SDC-1 binds IL-34 as a co-receptor with CSF-1R[55]. Intriguingly, all three known IL-34 receptors are expressed by Mø[55,56]. We now show that signaling through PTPRZ restricts Mø mediated inflammation in K/BxN serum-transfer arthritis. In contrast, blocking or inhibiting CSF-1R in arthritis models[14,15] is beneficial. By comparison, the role of Mø expressing SDC-1 in arthritis is less clear. In a recent study, delivering IL-34 into the joint using an adenoviral vector (adeno-IL-34) induced some features of arthritis by signaling through SDC-1[56]. However, there are concerns as to whether this model is faithful to the role of IL-34 in arthritis, for example, injecting adeno-IL-34 into the joint likely delivered pharmacologic, not physiologic levels of IL-34. Moreover, multiple studies indicate that SDC-1 promotes, rather than hinders repair in several tissues[57–59]. Of note, a connection between IL-34 and PTPRZ in RA was dismissed based on data showing PTPRZ expression is similar in RA, OA and normal controls[56]. As we have now shown, PTPRZ is elevated, tracks with disease activity and is integral in the pathogenesis of RA. Clearly, further studies are required to clarify the specific roles of CSF-1R, SDC-1 and PTPRZ in RA to guide treatment strategies.

In conclusion, IL-34 and PTPRZ-dependent Mø mediated mechanisms limit the severity of inflammatory arthritis with aspects similar to RA. These findings fuel further mechanistic studies necessary in the design of an IL-34 based therapeutic approach for patients with RA.

DATA AVAILABILITY

All data generated or analyzed during this study are included in this published article [and its supplementary information files].

REFERENCES

1. Chemel, M. et al. Interleukin 34 expression is associated with synovitis severity in rheumatoid arthritis patients. *Ann Rheum Dis* **71**, 150–154 (2012).
2. Hwang, S. J. et al. Interleukin-34 produced by human fibroblast-like synovial cells in rheumatoid arthritis supports osteoclastogenesis. *Arthritis Res Ther* **14**, R14 (2012).
3. Tian, Y., Shen, H., Xia, L. & Lu, J. Elevated serum and synovial fluid levels of interleukin-34 in rheumatoid arthritis: possible association with disease progression via interleukin-17 production. *J Interferon Cytokine Res* **33**, 398–401 (2013).
4. Zhang, F. et al. Interleukin-34 in rheumatoid arthritis: potential role in clinical therapy. *Int J Clin Exp Med* **8**, 7809–7815 (2015).
5. Carmona-Rivera C., et al. Neutrophil extracellular traps mediate articular cartilage damage and enhance cartilage component immunogenicity in rheumatoid arthritis. *JCI Insight.* **5**, e139388 (2020).
6. Wright, H. L., Lyon, M., Chapman, E. A., Moots, R. J. & Edwards, S. W. Rheumatoid arthritis synovial fluid neutrophils drive inflammation through production of chemokines, reactive oxygen species, and neutrophil extracellular traps. *Front Immunol* **11**, 584116 (2020).
7. Khandpur, R. et al. NETs are a source of citrullinated autoantigens and stimulate inflammatory responses in rheumatoid arthritis. *Sci Transl Med* **5**, 178ra140 (2013).
8. Takano, T. et al. Neutrophil survival factors (TNF-alpha, GM-CSF, and G-CSF) produced by macrophages in cats infected with feline infectious peritonitis virus contribute to the pathogenesis of granulomatous lesions. *Arch Virol* **154**, 775–781 (2009).
9. Wang, Y. et al. IL-34 is a tissue-restricted ligand of CSF1R required for the development of Langerhans cells and microglia. *Nat Immunol* **13**, 753–760 (2012).
10. Pollard, J. W. & Stanley, E. R. Pleiotropic roles for CSF-1 in development defined by the mouse mutation osteopetrotic (op). *Adv Dev Biochem* **4**, 153–193 (1996).
11. Campbell, I. K., Ianches, G. & Hamilton, J. A. Production of macrophage colony-stimulating factor (M-CSF) by human articular cartilage and chondrocytes. Modulation by interleukin-1 and tumor necrosis factor alpha. *Biochim Biophys Acta* **1182**, 57–63 (1993).
12. Nakano, K. et al. Rheumatoid synovial endothelial cells produce macrophage colony-stimulating factor leading to osteoclastogenesis in rheumatoid arthritis. *Rheumatology (Oxford)* **46**, 597–603 (2007).
13. Nandi, S. et al. Receptor-type protein-tyrosine phosphatase ζ is a functional receptor for interleukin-34. *J Biol Chem* **288**, 21972–21986 (2013).
14. Garcia, S. et al. Colony-stimulating factor (CSF) 1 receptor blockade reduces inflammation in human and murine models of rheumatoid arthritis. *Arthritis Res Ther* **18**, 75 (2016).
15. Paniagua, R. T. et al. c-Fms-mediated differentiation and priming of monocyte lineage cells play a central role in autoimmune arthritis. *Arthritis Res Ther* **12**, R32 (2010).
16. Christensen, A. D., Haase, C., Cook, A. D. & Hamilton, J. A. K/BxN serum-transfer arthritis as a model for human inflammatory arthritis. *Front Immunol* **7**, 213 (2016).
17. Monach, P. A., Mathis, D. & Benoist, C. The K/BxN arthritis model. *Curr Protoc Immunol* **Chapter 15**, Unit 15 22 (2008).
18. Shintani, T., Watanabe, E., Maeda, N. & Noda, M. Neurons as well as astrocytes express proteoglycan-type protein tyrosine phosphatase zeta/RPTPbeta: analysis of mice in which the PTPzeta/RPTPbeta gene was replaced with the LacZ gene. *Neurosci Lett* **247**, 135–138 (1998).
19. Fransen, J., Creemers, M. C. & Van Riel, P. L. Remission in rheumatoid arthritis: agreement of the disease activity score (DAS28) with the ARA preliminary remission criteria. *Rheumatology (Oxford)* **43**, 1252–1255 (2004).
20. Baek, J. H. et al. IL-34 mediates acute kidney injury and worsens subsequent chronic kidney disease. *J Clin Invest* **125**, 3198–3214 (2015).
21. Ajay, A. K. et al. A bioinformatics approach identifies signal transducer and activator of transcription-3 and checkpoint kinase 1 as upstream regulators of kidney injury molecule-1 after kidney injury. *J Am Soc Nephrol* **25**, 105–118 (2014).
22. Faust, J. et al. Correlation of renal tubular epithelial cell-derived interleukin-18 up-regulation with disease activity in MRL-Faslpr mice with autoimmune lupus nephritis. *Arthritis Rheum* **46**, 3083–3095 (2002).
23. Menke, J. et al. Colony-stimulating factor-1: a potential biomarker for lupus nephritis. *J Am Soc Nephrol* **26**, 379–389 (2015).
24. Wada, Y. et al. IL-34-dependent intrarenal and systemic mechanisms promote lupus nephritis in MRL-Fas lpr mice. *J Am Soc Nephrol* **30**, 244–259 (2019).
25. Glasson, S. S., Chambers, M. G., Van Den Berg, W. B. & Little, C. B. The OARSI histopathology initiative - recommendations for histological assessments of osteoarthritis in the mouse. *Osteoarthritis Cartilage* **18**, S17–S23 (2010).
26. Campbell, I. K. et al. Therapeutic targeting of the G-CSF receptor reduces neutrophil trafficking and joint inflammation in antibody-mediated inflammatory arthritis. *J Immunol* **197**, 4392–4402 (2016).
27. Pettit, A. R. et al. TRANCE/RANKL knockout mice are protected from bone erosion in a serum transfer model of arthritis. *Am J Pathol* **159**, 1689–1699 (2001).
28. O'Brien, W. et al. RANK-independent osteoclast formation and bone erosion in inflammatory arthritis. *Arthritis Rheumatol* **68**, 2889–2900 (2016).
29. Schett, G. & Gravallese, E. Bone erosion in rheumatoid arthritis: mechanisms, diagnosis and treatment. *Nat Rev Rheumatol* **8**, 656–664 (2012).
30. Sasmono, R. T. et al. Mouse neutrophilic granulocytes express mRNA encoding the macrophage colony-stimulating factor receptor (CSF-1R) as well as many other macrophage-specific transcripts and can transdifferentiate into macrophages in vitro in response to CSF-1. *J Leukoc Biol* **82**, 111–123 (2007).
31. Isozaki, T. et al. Evidence that CXCL16 is a potent mediator of angiogenesis and is involved in endothelial progenitor cell chemotaxis: studies in mice with K/BxN serum-induced arthritis. *Arthritis Rheum* **65**, 1736–1746 (2013).
32. Szekanecz, Z., Vegvari, A., Szabo, Z. & Koch, A. E. Chemokines and chemokine receptors in arthritis. *Front Biosci (Schol Ed)* **2**, 153–167 (2010).
33. Abdolmaleki, F. et al. The role of efferocytosis in autoimmune diseases. *Front Immunol* **9**, 1645 (2018).
34. Culemann, S. et al. Locally renewing resident synovial macrophages provide a protective barrier for the joint. *Nature* **572**, 670–675 (2019).
35. Grieshaber-Bouyer, R. et al. The neutrotime transcriptional signature defines a single continuum of neutrophils across biological compartments. *Nat Commun* **12**, 2856 (2021).
36. Agere, S. A., Akhtar, N., Watson, J. M. & Ahmed, S. RANTES/CCL5 induces collagen degradation by activating MMP-1 and MMP-13 expression in human rheumatoid arthritis synovial fibroblasts. *Front Immunol* **8**, 1341 (2017).
37. Darrah, E. & Andrade, F. NETs: the missing link between cell death and systemic autoimmune diseases? *Front Immunol* **3**, 428 (2012).
38. Radic, M. Clearance of apoptotic bodies, NETs, and biofilm DNA: implications for autoimmunity. *Front Immunol* **5**, 365 (2014).
39. Bratton, D. L. & Henson, P. M. Neutrophil clearance: when the party is over, clean-up begins. *Trends Immunol* **32**, 350–357 (2011).
40. Misharin, A. V. et al. Nonclassical Ly6C(-) monocytes drive the development of inflammatory arthritis in mice. *Cell Rep* **9**, 591–604 (2014).
41. Svendsen, P., Etzerodt, A., Deleuran, B. W. & Moestrup, S. K. Mouse CD163 deficiency strongly enhances experimental collagen-induced arthritis. *Sci Rep* **10**, 12447 (2020).
42. Foucher, E. D. et al. IL-34 induces the differentiation of human monocytes into immunosuppressive macrophages. antagonistic effects of GM-CSF and IFNγ. *PLoS One* **8**, e56045 (2013).
43. Liu, Y., Liu, H., Zhu, J. & Bian, Z. Interleukin-34 drives macrophage polarization to the M2 phenotype in autoimmune hepatitis. *Pathol Res Pract* **215**, 152493 (2019).
44. Schulz, D., Severin, Y., Zanotelli, V. R. T. & Bodenmiller, B. In-depth characterization of monocyte-derived macrophages using a mass cytometry-based phagocytosis assay. *Sci Rep* **9**, 1925 (2019).
45. Baghdadi, M. et al. High co-expression of IL-34 and M-CSF correlates with tumor progression and poor survival in lung cancers. *Sci Rep* **8**, 418 (2018).
46. Zhang, L. et al. Interleukin-34 aggravates the severity of arthritis in collagen-induced arthritis mice by inducing interleukin-17 production. *J Interferon Cytokine Res* **38**, 221–225 (2018).
47. Mizuno, T., Doi, Y., Mizoguchi, H., Jin, S., Noda, M. & Sonobe, Y. et al. Interleukin-34 selectively enhances the neuroprotective effects of microglia to attenuate oligomeric amyloid-β neurotoxicity. *Am J Pathol* **179**, 2016–2027 (2011).
48. Lin, X. et al. Interleukin-34 ameliorates survival and bacterial clearance in polymicrobial sepsis. *Crit Care Med* **46**, e584–e590 (2018).
49. Bézie, S. et al. IL-34 is a Treg-specific cytokine and mediates transplant tolerance. *J Clin Invest* **125**, 3952–3964 (2015).
50. Wang, B. et al. IL-34 upregulated Th17 production through increased IL-6 expression by rheumatoid fibroblast-like synoviocytes. *Mediators Inflamm* **2017**, 1567120 (2017).
51. Wang, B. et al. Increased IL-6 expression on THP-1 by IL-34 stimulation up-regulated rheumatoid arthritis Th17 cells. *Clin Rheumatol* **37**, 127–137 (2018).
52. Yang, S. et al. Interleukin 34 upregulation contributes to the increment of MicroRNA 21 expression through STAT3 activation associated with disease activity in rheumatoid arthritis. *J Rheumatol* **43**, 1312–1319 (2016).
53. Moon, S. J. et al. Increased levels of interleukin 34 in serum and synovial fluid are associated with rheumatoid factor and anticyclic citrullinated peptide antibody titers in patients with rheumatoid arthritis. *J Rheumatol* **40**, 1842–1849 (2013).
54. Chang, S. H. et al. Baseline serum interleukin-34 levels independently predict radiographic progression in patients with rheumatoid arthritis. *Rheumatol Int* **35**, 71–79 (2015).

55. Segaliny, A. I. et al. Syndecan-1 regulates the biological activities of interleukin-34. *Biochim Biophys Acta* **1853**, 1010–1021 (2015).
56. Van Raemdonck, K. et al. IL-34 reprograms glycolytic and osteoclastic RA macrophages via Syndecan-1 and M-CSFR. *Arthritis Rheumatol* **73**, 2003–2014 (2021).
57. Brauer, R. et al. Syndecan-1 attenuates lung injury during influenza infection by potentiating c-Met signaling to suppress epithelial apoptosis. *Am J Respir Crit Care Med* **194**, 333–344 (2016).
58. Celie, J. W. et al. Tubular epithelial syndecan-1 maintains renal function in murine ischemia/reperfusion and human transplantation. *Kidney Int* **81**, 651–661 (2012).
59. Jing, Z., Wei-Jie, Y., Yi-Feng, Z. G. & Jing, H. Downregulation of Syndecan-1 induce glomerular endothelial cell dysfunction through modulating internalization of VEGFR-2. *Cell Signal* **28**, 826–837 (2016).

ACKNOWLEDGEMENTS

We wish to acknowledge members of the Kelley lab, Taeyoung Lee, Hye Yoon Shin and Taichiro Minami for their excellence assisting with experiments. We want to thank Dr. Peter Nigrovic for his helpful suggestions and his laboratory for guidance learning the K/BxN serum-transfer arthritis model and members of the Franklin lab, Alan Baez Vazquez and Alicia Lai, for assistance with the in vitro phagocytosis experiment.

AUTHOR CONTRIBUTIONS

HMG-S, conducted experiments, acquired data, analyzed mouse data, and contributed to preparation of the manuscript; J-HB, conducted experiments, acquired data, analyzed mouse data, contributed to preparation of the manuscript; JW-M., conducted experiments, acquired, and analyzed mouse and human data and edited the manuscript, AKA, acquired mouse IP and Western blot data; JFC provided the radiology study and edited the manuscript, MN, provided breeding pair of PTPRZ KO mice and some advice, RAF, planned the phagocytosis experiments and edited the manuscript, PR-M assisted in planning and performed the phagocytosis assay, and VRK, planned and designed experiments, reviewed data and wrote the manuscript. All authors read and approved the final paper.

FUNDING

Rheumatology Research Foundation, Innovative Research Grant (VRK), the National Council on Science and Technology (CONACyT, Fellowships No. 252556 and 274369) (HMG-S), Basic Science Research Program through the National Research Foundation of Korea (NRF) funded by the Ministry of Education (2021R111A3059820) (J-H B), the Deutsche Forschungsgemeinschaft WE 5779/2-3 (JM-M) and the Harvard Stem Cell Institute (RAF).

COMPETING INTERESTS

VRK has an equity interest in Biogen-Idec, a company with research and development interests in lupus. VRK's interests were reviewed and are managed by the Brigham and Women's Hospital and MGB (Partners) HealthCare in accordance with conflicts of interest policy. The other authors have declared that no conflict of interest exist.

ETHICS APPROVAL

The use of human specimens was reviewed and approved by the Standing Committee for Clinical Studies of the Johannes-Gutenberg University in adherence to the Declaration of Helsinki (Approval No 837.467.13).

ADDITIONAL INFORMATION

Supplementary information The online version contains supplementary material available at https://doi.org/10.1038/s41374-022-00772-0.

Correspondence and requests for materials should be addressed to Vicki Rubin Kelley.

Reprints and permission information is available at http://www.nature.com/reprints

Publisher's note Springer Nature remains neutral with regard to jurisdictional claims in published maps and institutional affiliations.